





Article

Faraday's Efficiency Modeling of a Proton Exchange Membrane Electrolyzer Based on Experimental Data

Burin Yodwong ^{1,2}, Damien Guilbert ^{1,*}, Matheepot Phattanasak ², Wattana Kaewmanee ², Melika Hinaje ¹ and Gianpaolo Vitale ³

¹ Group of Research in Electrical Engineering of Nancy (GREEN), Université de Lorraine, GREEN, F-54000 Nancy, France; burin.yodwong@univ-lorraine.fr (B.Y.); melika.hinaje@univ-lorraine.fr (M.H.)

² Department of Teacher Training in Electrical Engineering, King Mongkut's University of Technology North Bangkok (KMUTNB), Bangkok 10800, Thailand; matheepot.p@fte.kmutnb.ac.th (M.P.); wattana.k@fte.kmutnb.ac.th (W.K.)

³ Institute for High Performance Computing and Networking (ICAR), National Research Council of Italy, Unit of Palermo, 90146 Palermo, Italy; gianpaolo.vitale@icar.cnr.it

* Correspondence: damien.guilbert@univ-lorraine.fr

Received: 21 August 2020; Accepted: 9 September 2020; Published: 14 September 2020



Abstract: In electrolyzers, Faraday's efficiency is a relevant parameter to assess the amount of hydrogen generated according to the input energy and energy efficiency. Faraday's efficiency expresses the faradaic losses due to the gas crossover current. The thickness of the membrane and operating conditions (i.e., temperature, gas pressure) may affect the Faraday's efficiency. The developed models in the literature are mainly focused on alkaline electrolyzers and based on the current and temperature change. However, the modeling of the effect of gas pressure on Faraday's efficiency remains a major concern. In proton exchange membrane (PEM) electrolyzers, the thickness of the used membranes is very thin, enabling decreasing ohmic losses and the membrane to operate at high pressure because of its high mechanical resistance. Nowadays, high-pressure hydrogen production is mandatory to make its storage easier and to avoid the use of an external compressor. However, when increasing the hydrogen pressure, the hydrogen crossover currents rise, particularly at low current densities. Therefore, faradaic losses due to the hydrogen crossover increase. In this article, experiments are performed on a commercial PEM electrolyzer to investigate Faraday's efficiency based on the current and hydrogen pressure change. The obtained results have allowed modeling the effects of Faraday's efficiency by a simple empirical model valid for the studied PEM electrolyzer stack. The comparison between the experiments and the model shows very good accuracy in replicating Faraday's efficiency.

Keywords: PEM electrolyzer; Faraday's efficiency; faradaic losses; crossover current; hydrogen flow rate; energy efficiency; modeling; gas pressure

1. Introduction

To face the depletion of fossil fuels (i.e., oil, natural gas) and the reduction of the greenhouse gas emission, decarbonized hydrogen production pathways based on renewable energy sources (i.e., wind energy, photovoltaic energy, hydro energy) and water electrolysis are considered attractive and promising solutions for a sustainable future [1,2]. In these pathways, generated and stored hydrogen can be employed for different applications such as transportation, energy storage, power-to-gas, and industry [1,3]. The water electrolysis process consists of employing electricity generated from renewable energy sources to split pure water into oxygen and hydrogen [4]. It is performed by electrolyzers. Currently, different types of electrolyzer exist depending on the type of electrolyte used and charge carrier such as alkaline, proton exchange membrane (PEM) and solid oxide (SO) [5,6].

Nevertheless, alkaline and PEM are the only technologies that can be found in the market; the SO technology is still in the research and development phase because of its recent introduction [4]. Since the principle of alkaline water electrolysis is well known (first introduced more than 200 years ago), this technology has been deployed all over the world, meeting the requirements for power-to-gas and industrial applications [7,8]. Indeed, the available stack power can reach a few megawatts. On one hand, the main advantages of this technology are low-cost catalysts, having a higher lifetime, and gas purity. On the other hand, this technology features several disadvantages in terms of low current density, flexibility, ohmic loss, and operating pressure [7]. Their penetration in markets of great potential is limited to their partial load range. Generally, it is included between 40–100% but some manufacturers such as NEL have developed alkaline electrolyzers with a partial load range of 15–100% [2]. The partial load range is an important issue when coupling electrolyzers with renewable energy sources to ensure decarbonized hydrogen production. Since renewable energy sources are very dynamic sources, the electrolyzers must be able to absorb the energy during dynamic operation and even at low wind speed [9]. However, the limited partial load range and low current densities of alkaline electrolyzers make them less efficient during dynamic operation. In comparison, PEM electrolyzers feature high current densities (above $2 \text{ A}\cdot\text{cm}^{-2}$), as well as a high power density, small footprint, high efficiency, very thin membrane (i.e., 25–254 μm), high-pressure operation, and fast response to dynamic operations, which makes it perfectly fit when connecting with renewable energy sources [4,5]. However, this technology suffers from high cost due to the use of costly catalyst materials (e.g., iridium, platinum) both at the anode and the cathode; this slows down large scale use and market penetration compared to alkaline electrolyzers [4,5].

In electrolyzers, to evaluate their performance from the amount of hydrogen produced and energy efficiency point of view, the Faraday's efficiency, commonly called current efficiency, is a challenging issue [10]. In fact, it allows for describing the fraction between the amount of hydrogen generated and the theoretical hydrogen amount which could be generated according to the electrical energy input [10]. It is important to point out that Faradaic losses are due to shunt currents introduced by the design of bipolar plate materials of electrolyzers. These shunt currents bypass into current collectors in the electrolyzer stack [11]. They can be evaluated by the ratio between measured and theoretical gas flow rate. The gas flow rate measurement is carried out through a bubble flowrate meter [12]. In the literature, many papers have been reported to investigate and predict shunt currents in electrochemical devices such as batteries [13,14] and electrolyzers [11,12,15].

The first investigations on Faraday's efficiency have been introduced for alkaline water electrolysis in the 1990s by Hug et al. [15] and Ulleberg [16]. They have demonstrated that the Faradaic losses increase at low current densities due to lower electrolyte resistance. From experiments, they have developed empirical expressions to model the Faraday's efficiency based on the input current and temperature change. A growth in temperature causes a lower electrical resistance since the electrolyte is sensitive to temperature change [10]. As a result, the Faraday's efficiency decreases when increasing the temperature. In [17], the authors analyzed the effects of operating temperature and membrane thickness on the Faraday's efficiency for a PEM electrolyzer. Nevertheless, they have not developed a model to assess Faraday's efficiency. Based on the first works introduced in [15,16], Faraday's efficiency has been reported in several works for modeling purposes both for alkaline and PEM electrolyzers [18–27]. Nonetheless, this model is only valid for alkaline electrolyzers and cannot be employed to the PEM electrolyzer because of their different materials used for their manufacturing (e.g., membrane). In general, the proposed models for alkaline electrolyzers are characterized by some parameters that have to be identified based on the electrolyzer, the temperature appears explicitly as a variable, differently the pressure is assumed as constant; as a consequence, it is hidden inside the parameters.

From the current state-of-the-art, it can be highlighted that a few works have been carried out on the Faraday's efficiency investigation for PEM electrolyzers. Besides, no models depending on the hydrogen pressure have been proposed either for alkaline or PEM electrolyzers. Hence, the objective

of this article is to assess the effects of the input current and hydrogen pressure on the Faraday's efficiency. This analysis aims to describe the behavior of the electrolyzer in the low-density current zone; here varying the current the temperature shows low variations since losses are reduced, and that contrarily, the influence of the pressure of the efficiency curve is relevant. The investigation is based on experiments carried out with a commercial PEM electrolyzer. The obtained results have enabled developing a simple empirical expression valid for the PEM stack electrolyzer studied to model the Faraday's efficiency based on the current and hydrogen pressure change. The comparison between the experiments and the proposed model demonstrate the exactness of the model in reproducing the Faraday's efficiency according to the operating conditions. Faraday's efficiency model can be helpful to determine the energy efficiency of the electrolyzer based on the cell voltage efficiency. Cell voltage efficiency can be assessed by dividing the thermoneutral voltage (i.e., 1.291 V) by the voltage of each cell. It quantifies the effects of cell polarization. In the literature, Faraday's efficiency is usually considered equal to 1 and consequently, the energy efficiency does not take into consideration gas crossover losses.

This article is divided into four sections. After this introduction emphasizing the current state-of-the-art and reasons to carry out this work, Section 2 summarizes the main contributions of the investigation and modeling of the Faraday's efficiency of alkaline and PEM electrolyzers. Then, in Section 3, the realized test bench to carry out experiments is presented. Besides, different tests at different hydrogen pressure are performed to analyze their effects on the Faraday's efficiency for modeling purposes. Finally, in Section 4, a discussion is provided to compare the experiments and the developed model and then conclusions about its effectiveness. Furthermore, future challenges in enhancing the Faraday's efficiency are given.

2. Research Background

The performance of the electrolyzers are strongly linked with the hydrogen flow rate, \dot{N}_{H_2} , and energy efficiency, η_{el} , which are expressed by the following expression [10]:

$$\dot{N}_{H_2} = \frac{\eta_F n_c i_{el}}{zF} \quad (1)$$

$$\eta_{el} = \eta_v \eta_F = \frac{\Delta H \dot{N}_{H_2}}{v_{el} i_{el}} \quad (2)$$

Faraday's efficiency defines the fraction between the generated quantity of hydrogen (H_2) and the theoretical hydrogen quantity which could be produced according to the electrical energy input.

The electrolyzer current is the same in each of the electrolysis cells and consequently, the calculated gas volume is produced in each of the cells. Hence, the theoretical hydrogen quantity must be multiplied by the number of cells n_c .

Faraday's efficiency influences the variation of the hydrogen for given current variation. When this curve asymptotically tends to the unitary value, the derivative is approximately null and a current variation around the operating point produces the same hydrogen variation. Contrarily, when the efficiency drops, as in the low current zone, the same increase or decrease of the current produces different changes on the hydrogen. This phenomenon is emphasized when the supply current is obtained by rectifiers since the DC current contains a low-frequency ripple superimposed.

From Equations (1) and (2), it can be noted that the Faraday's efficiency affects both hydrogen flow rate and energy efficiency. By inserting Equation (1) into Equation (2), the following expression is obtained:

$$\eta_{el} = \left(\frac{\Delta H n_c}{zF} \right) \frac{\eta_F}{v_{el}} \quad (3)$$

The terms appearing in the brackets are considered constants, whereas the variables are the Faraday's efficiency and the stack voltage. Faradaic losses are particularly distinct at low

current densities. For this reason, energy efficiency is strongly affected by the stack voltage. The higher the stack voltage, the lower the energy efficiency.

According to the second Faraday's law of electrolysis and the general gas equation, the theoretical hydrogen quantity can be determined:

$$V_{H_2}(\text{calculated}) = \frac{R \cdot i_{el} \cdot t \cdot T}{F \cdot p \cdot z} \quad (4)$$

On the one hand, the Faraday's efficiency is greater than the energy efficiency (2), since it only takes into consideration the losses due to the gas crossover [10]. On the other hand, energy efficiency takes into consideration additional losses such as ohmic losses and joule losses both at the anode and cathode. Since the 1990s, a few works have been published in the literature on the analysis and the modeling of Faraday's efficiency [10,15,16]. The works are mainly focused on alkaline electrolyzers and two empirical models have been reported in the 1990s to model Faraday's efficiency based on the input current of the electrolyzer and temperature. The first empirical model was developed by Hug et al. [15] in 1993; whereas the second model by Ulleberg [16] in 1998. The first empirical model developed by Hug et al. [15] includes five parameters as follows:

$$\eta_F = B_1 + B_2 \exp \frac{B_3 + B_4 T + B_5 T^2}{i_{el}} \quad (5)$$

This empirical model can provide a good accuracy of Faraday's efficiency, whatever the temperature and the current. Experimental data at different temperatures are required to determine the five parameters of the model.

By comparison, Ulleberg first proposed an empirical model on seven parameters described by [16]:

$$\eta_F = a_1 \exp \left(\frac{a_2 + a_3 T + a_4 T^2}{\frac{i_{el}}{A}} + \frac{a_5 + a_6 T + a_7 T^2}{\left(\frac{i_{el}}{A}\right)^2} \right) \quad (6)$$

where A is the active area in (m^2) of the electrolyzer. To evaluate the seven parameters, experimental tests have been carried out at different temperatures (i.e., 40 °C, 60 °C, and 80 °C) on an HYSOLAR alkaline electrolyzer (10 kW, 5 bar, 0.05 m^2 , 25 cells). The obtained parameters are reported in [16]. To highlight the effect of the temperature on the Faraday's efficiency, it has been plotted according to the current density at different temperatures in Figure 1.

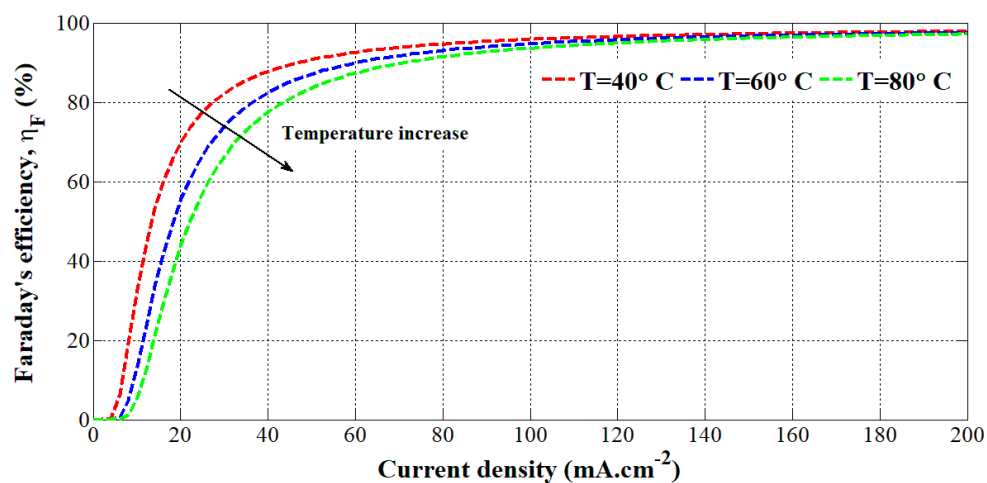


Figure 1. Faraday's efficiency according to the current density at different temperatures.

It can be emphasized that the higher the temperature, the lower the Faraday's efficiency since the electrolyte resistance is lower, leading up to higher crossover currents. This model has been employed in [28] to evaluate the hydrogen flow rate based on the temperature and current.

The model (11) has been then simplified by Ulleberg with only four parameters:

$$\eta_F = \frac{\left(\frac{i_{\text{cell}}}{A}\right)^2}{f_{11} + (f_{12} \cdot T) + \left(\frac{i_{\text{cell}}}{A}\right)^2} \cdot (f_{21} + (f_{22} \cdot T)) \quad (7)$$

The four parameters can be evaluated based on experimental data at different temperatures. Finally, in [10], the Faraday's efficiency depends on two parameters for a given temperature:

$$\eta_F = \frac{\left(\frac{i_{\text{cell}}}{A}\right)^2}{f_1 + \left(\frac{i_{\text{cell}}}{A}\right)^2} \cdot f_2 \quad (8)$$

The parameters of this model have been reported for a PHOEBUS electrolyzer (26 kW, 7 bar, $T = 80 \text{ }^\circ\text{C}$, 0.25 m^2 , 21 cells) and an HYSOLAR alkaline electrolyzer (10 kW, 5 bar, $T = 80 \text{ }^\circ\text{C}$) and are summarized in [10,16].

From these parameters reported for both alkaline electrolyzers, Faraday's efficiency has been plotted versus the current density in Figure 2. It can be underlined that both Faraday's efficiencies are similar at low current densities but from a current density of $20 \text{ mA}\cdot\text{cm}^{-2}$, the HYSOLAR alkaline electrolyzer shows a higher Faraday's efficiency than the PHOEBUS alkaline electrolyzer. It can be explained by the fact that the gas pressure of the HYSOLAR electrolyzer is smaller than that of the PHOEBUS electrolyzer. The consequence of gas pressure on Faraday's efficiency has been introduced in previous works [29–31] where an increase in gas pressure decreases Faraday's efficiency.

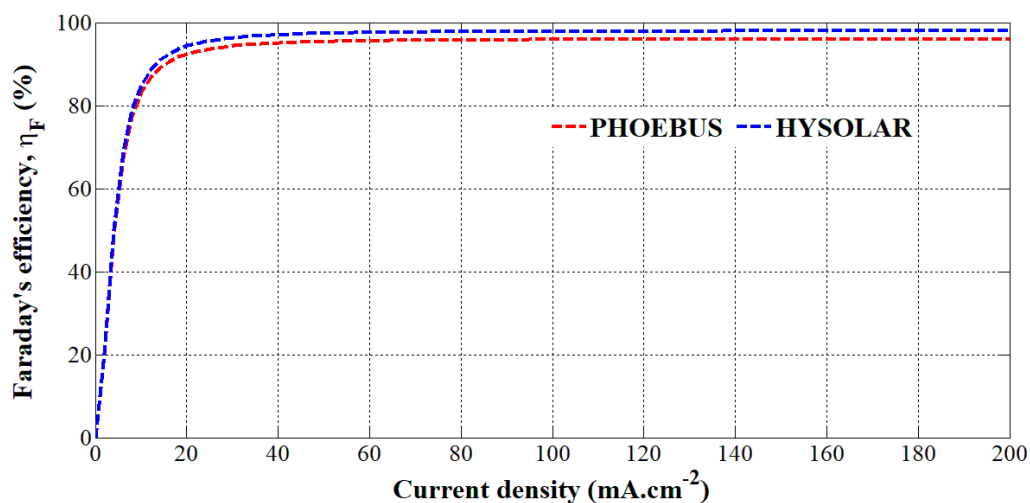


Figure 2. Faraday's efficiency versus the current density for the PHOEBUS and HYSOLAR alkaline electrolyzers.

It should be remarked that even if the Faraday's efficiency is often sketched at constant temperature, it does not represent the real operation of the electrolyzer. In fact, higher currents imply an increase in the temperature due to the losses.

The model (8) has been used in [26,27] to obtain the hydrogen flow rate for a given temperature.

Conversely, based on the work carried out by Ulleberg in [16], many authors have employed this following expression to determine the Faraday's efficiency at a given temperature (40 °C) [18–24]:

$$\eta_F = 96.5 \exp\left(\frac{0.09}{i_{el}} - \frac{75.5}{i_{el}^2}\right) \quad (9)$$

This model has been obtained from experiments performed on a PHOEBUS electrolyzer (26 kW, 7 bar, T = 40 °C, 0.25 m², 21 cells) [10]. The Faraday's efficiency given by Equation (9) has been plotted according to the current density in Figure 3.

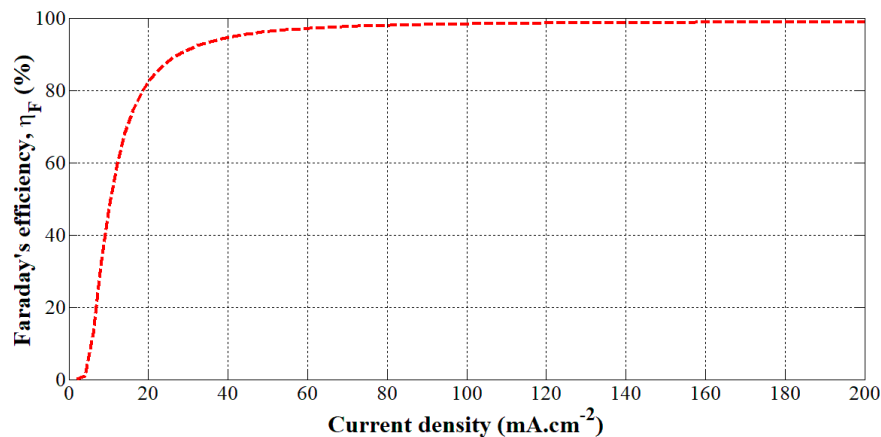


Figure 3. Faraday's efficiency versus the current density for a given temperature (40 °C).

Finally, in [17,29–31], compared to results reported in [10,15,16] for alkaline electrolyzers, the authors have shown that the temperature slightly affects the Faraday's efficiency of PEM electrolyzers. However, membrane thickness and gas pressure have a strong influence on the Faraday's efficiency. On the one hand, the greater the gas pressure, the smaller the Faraday's efficiency. On the other hand, the thinner the membrane thickness, the higher the crossover currents. As a result, membrane thickness and operating pressures are challenging issues to improve the efficiency of PEM electrolyzers [29–31].

3. Study of the Faraday's Efficiency

3.1. Description of the Experimental Test Bench

To analyze the Faraday's efficiency versus the current and gas pressure change, an experimental test rig has been realized at the GREEN laboratory (IUT de Longwy, France) as shown in Figure 4.

The test bench includes the following devices: (1) PEM electrolyzer, (2) H₂ flow rate meter from Bronkhorst Company, (3) a current clamp, (4) a voltage probe, (5) 4-channel oscilloscope, (6) DC power supply from EA Elektro-Automatik Company, (7) a laptop with a virtual control panel to control the DC power supply, and (8) a pressurized pure water tank. The generated hydrogen is stored in three metal hydride tanks (not shown in Figure 4). The investigated PEM electrolyzer is NMH2 1000 from HELIOCENTRIS Company, the technical data of which are reported in Table 1. In this work, only the PEM electrolyzer stack is employed to be connected to an external DC power supply. The experimental data of the H₂ flow rate collected by the H₂ flow rate meter are transferred to a laptop through an RS-232/USB connection. The H₂ flow rate is provided in (Nm³.h⁻¹).

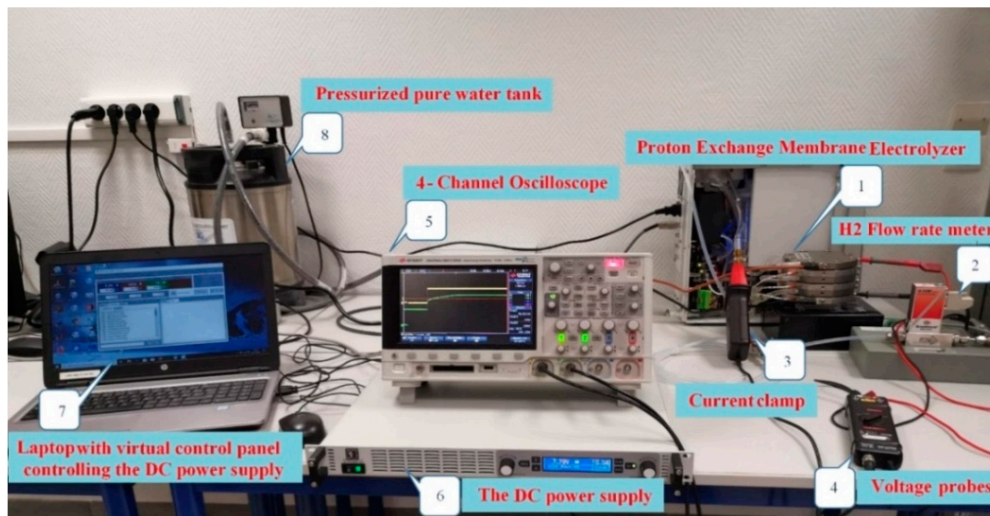


Figure 4. Realized experimental test bench in laboratory.

Table 1. Technical data of the investigated PEM EL.

Parameters	Value	Unit
Rated electrical power	400	W
Stack operating voltage range	4.4–8	V
Stack current range	0–50	A
Delivery output pressure	0.1–10.5	bar
Cells number	3	-
Active area Section	50	cm ²
Membrane thickness	25.4	µm

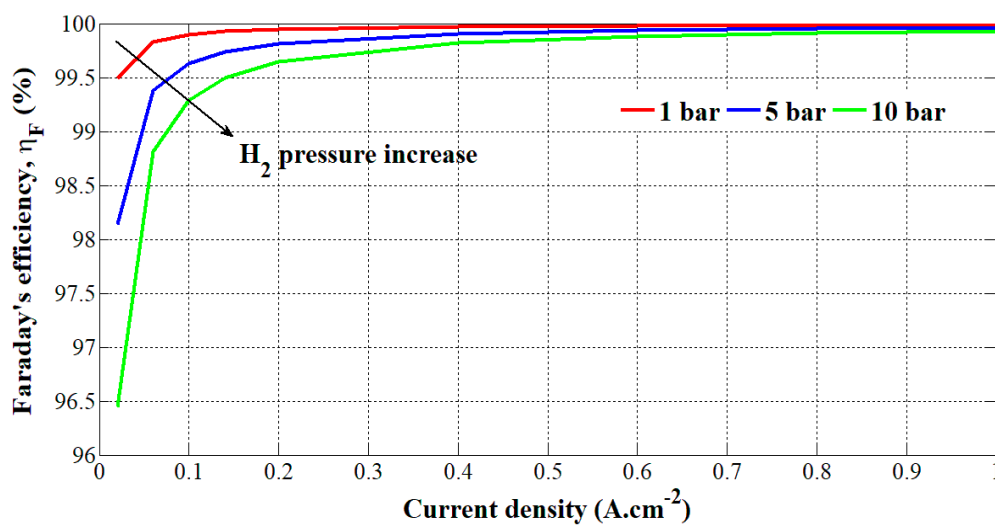
The hydrogen delivery output pressure can be set through the software from HELIOCENTRIS Company with an RS-232 connection. In comparison, the oxygen delivery output pressure is set to one bar.

3.2. Analysis of the Faraday's Efficiency Based on the Cathode Gas Pressure Change

Through the realized test bench in Figure 4, experimental tests have been carried out at different hydrogen pressures (i.e., 1, 5, and 10 bar) and current densities (from 0 to 1 A.cm⁻²). The current is applied to the PEM electrolyzer through the DC power supply controlled by a laptop. The theoretical hydrogen flow rate has been calculated by using Equation (9) and multiplying it by the number of cells (i.e., 3). The obtained values in (m³.s⁻¹) have been multiplied by 60s and 1000 to get a theoretical hydrogen flow rate in (slpm (standard liter per minute)). In comparison, regarding the experimental hydrogen flow rate given in (Nm³.h⁻¹), it has been converted into (slpm). Finally, the Faraday's efficiency is obtained by applying Equation (4). The obtained results are summarized in Table 2. Faraday's efficiency versus the current density and hydrogen pressure change is shown in Figure 5.

Table 2. Theoretical and experimental hydrogen flow rate for a hydrogen pressure of 1,5, and 10 bar.

i_{el} (A)	1 Bar.			5 Bar.			10 Bar.		
	V_{H2exp}	V_{H2th}	η_F	V_{H2exp}	V_{H2th}	η_F	V_{H2exp}	V_{H2th}	η_F
1	0.0226	0.0227	0.9949	0.0044	0.0045	0.9814	0.0022	0.0023	0.9644
3	0.0681	0.0682	0.9983	0.0136	0.0136	0.9938	0.0067	0.0068	0.9881
5	0.1136	0.1137	0.9990	0.0226	0.0227	0.9963	0.0113	0.0114	0.9929
7	0.1590	0.1591	0.9993	0.0317	0.0318	0.9973	0.0158	0.0159	0.9949
10	0.2272	0.2273	0.9995	0.0454	0.0455	0.9981	0.0227	0.0227	0.9964
20	0.4546	0.4547	0.9997	0.0909	0.0909	0.9991	0.0454	0.0455	0.9982
30	0.6819	0.6820	0.9998	0.1363	0.1364	0.9994	0.0681	0.0682	0.9988
40	0.9093	0.9094	0.9999	0.1818	0.1819	0.9995	0.0909	0.0909	0.9991
50	1.1366	1.1367	0.9999	0.2273	0.2273	0.9996	0.1136	0.1137	0.9993

**Figure 5.** Obtained Faraday's efficiency based on current density and hydrogen pressure change.

The error on V_{H_2} measurement is ± 0.0001 slpm. Based on Figure 5, it can be noted that the Faraday's efficiency is relatively high ($> 96\%$). High Faraday's efficiency can be explained by the fact that recently, PEM electrolyzers have been designed with technical improvements compared to the Faraday's efficiency obtained for alkaline electrolyzers in the 1990s. By increasing the hydrogen output pressure, the Faraday's efficiency is lower due to higher crossover currents through the membrane, corroborating the results obtained in previous works [29–31]. The effects of higher pressures are particularly noticeable at low current densities; whereas from 25 A (i.e., 0.5 A.cm^2), Faraday's efficiency is similar for the three tests. Currently, the commercial PEM electrolyzers can generate hydrogen up to 35 bar. At that pressure, the Faradaic losses are higher. Over recent years, many researchers and companies have been working on increasing the hydrogen output pressure (>100 bar) to avoid the use of an external hydrogen compressor from the cost and energy efficiency issues. Indeed, the production of pressurized hydrogen could make easier its transportation and the growth of hydrogen refueling stations for fuel cell electric vehicles. The increase in pressure has been made possible due to the use of thinner membranes in PEM electrolyzers (i.e., high mechanical resistance) and new materials (i.e., zinc) at the anode and cathode [2–4]. Given that higher pressures lead up to the decrease of Faraday's efficiency and energy efficiency as well, the hydrogen pressure and membrane thickness are challenging issues and must be optimized to enhance the energy efficiency of the electrolyzer [31]. To optimize the Faraday's efficiency, some authors [32,33] have proposed to control power electronic converters connected to a PEM electrolyzer for specific operating conditions (i.e., stack voltage and current).

3.3. Mathematical Modeling of the Faraday's Efficiency

Based on the results reported in Table 2, the authors propose for the first time a fit empirical equation to model the Faraday's efficiency versus the current and hydrogen pressure change. The model has been devised considering the current density multiplied by a quantity depending on the pressure. To take into consideration nonlinear behavior, the current density has an exponent to be determined based on the pressure. First, by using the experimental data (i.e., current density, Faraday's efficiency), the most suitable empirical expression has been found by using the curve-fitting tool of Matlab/Simulink (2020a, MathWorks, Natick, Massachusetts, USA) software. The empirical expression is based on a power equation including two terms as follows:

$$\eta_F = a \left(\frac{i_{el}}{A} \right)^b + c \quad (10)$$

where A is the cross section of the studied PEM electrolyzer (m^2) and a , b , and c are parameters to evaluate. By employing a least-square regression algorithm and the experimental data for different hydrogen pressure, the parameters of the empirical Equation (10) have been assessed. The parameters are summarized in Table 3.

Table 3. Parameters of the empirical model according to the hydrogen pressure.

p (Bar)	a	b	c
1	-0.005103	-1	1
5	-0.01871	-1	1
10	-0.03572	-1	1

From Table 3, it can be noted that only the parameter a is dependent on the pressure. The value of the exponent b shows that the higher the current, the lower the efficiency expected. Hence, the next objective is to find a suitable expression to take into consideration the effect of the hydrogen pressure on parameter a . In Figure 6, parameter a is plotted according to the hydrogen pressure. From Figure 6, parameter a varies linearly according to the hydrogen pressure. The higher the pressure, the smaller the parameter a . Thus, it can be modeled as a linear expression:

$$a = a_1 p + a_2 \quad (11)$$

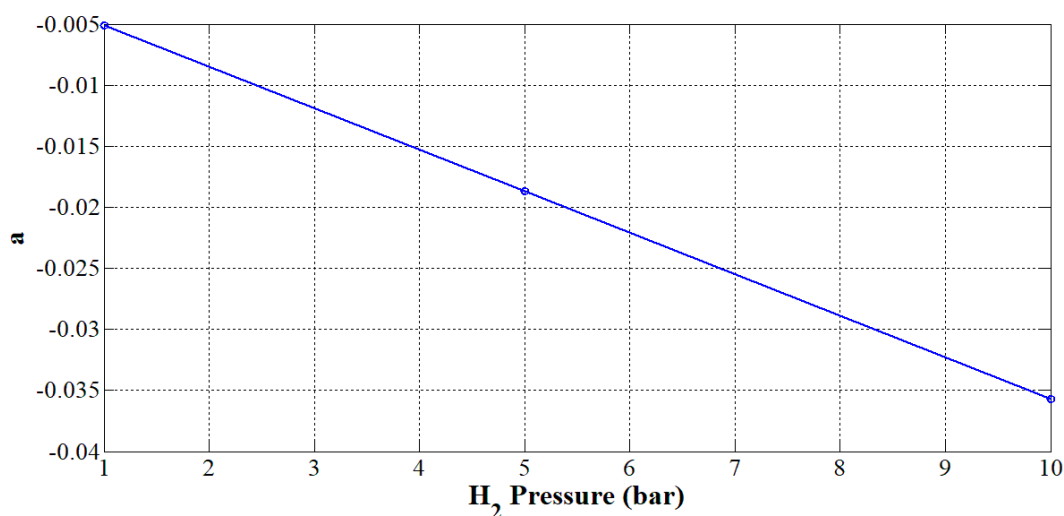


Figure 6. Effect of the hydrogen pressure on parameter a .

By using the command polyfit of Matlab/Simulink software and the data given in Table 2, the parameters a_1 and a_2 have been determined and are given in Table 4.

Table 4. Parameters of the linear model.

a_1	a_2
-0.0034	-0.001711

In summary, by substituting Equation (11) into Equation (10), the complete empirical model can be obtained:

$$\eta_F = (a_1 p + a_2) \left(\frac{i_{el}}{A} \right)^b + c \quad (12)$$

3.4. Validation of the Developed Models

The empirical model obtained in Equation (12) has been compared to the experimental data at different hydrogen pressure. The comparison is shown in Figure 7. It can be underlined that the model enables replicating precisely Faraday's efficiency versus the current density and hydrogen pressure change. It highlights the drop of efficiency for low current density. In conclusion, the developed model can be helpful to determine accurately the hydrogen flow rate and energy efficiency in accordance with the operating conditions.

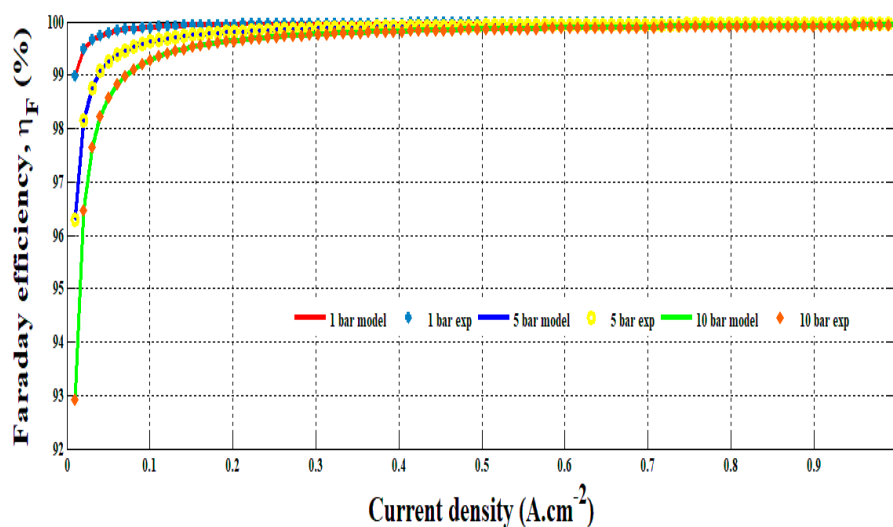


Figure 7. Comparison of the experiments and the model for 1, 5 and 10 bar.

4. Discussion and Future Challenges

The first investigations on Faraday's efficiency of an alkaline electrolyzer were reported in the 1990s. These studies have enabled modeling the effect of current density and temperature on the Faraday's efficiency by using empirical equations. Based on the current literature, Ulleberg's model is often used to assess the hydrogen flow rate and energy efficiency for a provided temperature. Recently, several studies have been reported to demonstrate the effect of membrane thickness and gas pressure on Faraday's efficiency. Temperature, membrane thickness, and gas pressure are relevant data affecting the performance of the electrolyzers. However, no models have been proposed on recent electrolyzers, that demonstrate technical improvements compared to the electrolyzers in the 1990s. For this reason, this preliminary work offers a new contribution about the modeling of Faraday's efficiency according to current density and hydrogen pressure change.

The obtained empirical model is simple and includes a few parameters, which can be obtained by employing a least-square algorithm. The comparison between the experimental measurements

and the developed model demonstrates the accuracy of the model in reproducing Faraday's efficiency according to current density and hydrogen pressure change. However, due to the use of a small-scale electrolyzer, the hydrogen pressure is set to 10 bar; whereas some commercial electrolyzer models can produce pressurized hydrogen up to 30 bar. At that pressure, the faradaic losses are higher due to higher crossover currents as shown in the scientific literature [25–27]. In this case, the model proposed is still valid but a new identification of the parameters is required. To highlight the contribution of this work, a comparative summary reported in Table 5 has been realized to summarize the main characteristics of the reported models in the literature and the proposed model.

Table 5. Comparison between the previously reported models and proposed model.

Model	Electrolyzer	Number of Parameters	Temperature Dependence	Pressure Dependence
Hug [11]	Alkaline	5	Yes	No
Ulleberg [12]	Alkaline	7	Yes	No
Ulleberg [10]	Alkaline	4	Yes	No
Proposed	PEM	4	No	Yes

The method proposed in this paper is a “black box” approach in which the main parameters, such as current, pressure, and temperature are considered, taken at the electrolyzer's external terminals. These parameters are supposed to be uniform inside the electrolyzer; for example, the current density is obtained by dividing the current for the surface. Of course, it is an approximation; however, it is useful to achieve the proposed model. In general, a nonuniform distribution of the current worsens the performance; hot-spots can be created with consequent over-heating. Besides, if the flow is disturbed by parasitic paths, energy conversion efficiency into hydrogen molecules is lowered. The Faraday's efficiency is influenced by the nonuniformity of the distribution of the current and potential as explained in [12] and of shunt current [11] depending on the presence of separators and electrodes shape. The knowledge of these phenomena requires a study taking into account the internal model of the electrochemical reactor. Some endeavors are proposed by literature; the current distribution can be improved by a suitable choice of flow paths [34,35]; these studies showed that it is possible to devise a good model of flows inside electrochemical reactors, and it is confirmed by experimental validation [36]. It is important to underline that the above-mentioned studies can be used for general problems taking into account concentration or conductivity variations and helps the designer in scale-up situations. The Faraday's efficiency can be further improved by combining the proposed “black-box” approach and the analysis presented in the literature.

In the future, to face hydrogen storage and refueling issues, the production of hydrogen at high-pressure is a key issue. Indeed, it allows for making hydrogen storage easier in tanks and improving its refueling in fuel cell electric vehicles. Furthermore, it avoids the use of an external compressor, responsible for increasing the overall cost and decreasing energy efficiency. As a result, since higher operating pressure leads up to the decrease of Faraday's efficiency, technical improvements in designing electrolyzers must be brought [31].

5. Conclusions

The main aim of this article was to analyze and model Faraday's efficiency in accordance with the current density and hydrogen pressure. It was demonstrated that Faradaic losses are noticeable at low current densities and a growth in hydrogen pressure led up to the decrease of Faraday's efficiency. A simple empirical model has been proposed based on a few parameters, which can be assessed by employing a least-square regression algorithm. The obtained results in comparing the experimental data and the model have allowed for validating the precision of the model in reproducing Faraday's efficiency in compliance with the operating conditions.

Based on this preliminary work, additional studies are needed to analyze how the coefficients of the model vary comparing different PEM electrolyzers and to investigate thoroughly the consequences of high-pressure operation on Faraday's efficiency and to model it. These models can be helpful for researchers and industry to optimize the efficiency of the electrolyzers in accordance with the operating conditions.

Author Contributions: Conceptualization, B.Y., D.G., M.P., W.K., M.H., and G.V.; methodology, B.Y., D.G., M.P., W.K., M.H., and G.V.; validation, B.Y. and D.G.; investigation, B.Y. and D.G.; writing—original draft preparation, D.G.; writing—review and editing, B.Y. and D.G. All authors have read and agreed to the published version of the manuscript.

Funding: This research received no external funding.

Acknowledgments: The authors are very grateful to the French Embassy in Bangkok (Thailand) and Campus France in funding Burin Yodwong's Ph.D. Thesis within the framework of the Franco-Thai scholarship program. Furthermore, the authors would like to address a special thanks to the GREEN laboratory of the Université de Lorraine and Thai-French Innovation Institute of King Mongkut's University of Technology North Bangkok for their constant encouragement and support in promoting research collaboration between France and Thailand. This work was supported by King Mongkut's University of Technology North Bangkok. Contract no. KMUTNB-GOV-58-58.

Conflicts of Interest: The authors declare no conflict of interest.

Abbreviations

The following abbreviations are used in this manuscript.

PEM	proton exchange membrane
SO	solid oxide

Nomenclature

The following abbreviations are used in this manuscript.

\dot{N}_{H_2}	Hydrogen flow rate (mol.s ⁻¹ or slpm)
η_{el}	energy efficiency
η_F	Faraday's efficiency
n_c	Number of the electrolyzer cells
i_{el}	Electrolyzer current (A)
z	Number of electrons exchanged during the reaction
F	Faraday's constant ($F = 96485 \text{ C.mol}^{-1}$)
η_v	Cell voltage efficiency
ΔH	Hydrogen higher heating value ($\Delta H = 286,000 \text{ Joule}$)
v_{el}	Stack voltage (V)
v_{cell}	Cell voltage (V)
V_{H_2}	Hydrogen volume (m ³)
η_{el}	Electrolyzer efficiency
t	Total time the constant current has been applied (s)
p	Ambient pressure (Pa)
R	Universal gas constant ($R = 8.314 \text{ J. mol}^{-1}. \text{ K}^{-1}$)
T	Ambient temperature (K)

References

1. Buttler, A.; Spliethoff, H. Current status of water electrolysis for energy storage, grid balancing and sector coupling via power-to-gas and power-to-liquids: A review. *Renew. Sustain. Energy Rev.* **2018**, *82*, 2440–2454. [[CrossRef](#)]
2. Carmo, M.; Stolten, D. Energy Storage Using Hydrogen Produced From Excess Renewable Electricity. In *Science and Engineering of Hydrogen-Based Energy Technologies*; Elsevier: Amsterdam, The Netherlands, 2019; pp. 165–199.
3. Wulf, C.; Linssen, J.; Zapp, P. Power-to-Gas—Concepts, Demonstration, and Prospects. In *Hydrogen Supply Chains*; Elsevier: Amsterdam, The Netherlands, 2018; pp. 309–345.

4. Hiva Kumar, S.; Himabindu, V. Hydrogen production by PEM water electrolysis—A review. *Mater. Sci. Energy Technol.* **2019**, *2*, 442–454. [[CrossRef](#)]
5. Carmo, M.; Fritz, D.L.; Mergel, J.; Stolten, D. A comprehensive review on PEM water electrolysis. *Int. J. Hydrog. Energy* **2013**, *38*, 4901–4934. [[CrossRef](#)]
6. Falcão, D.; Pinto, A. A review on PEM electrolyzer modelling: Guidelines for beginners. *J. Clean. Prod.* **2020**, *261*, 121184. [[CrossRef](#)]
7. David, M.; Ocampo-Martínez, C.; Sánchez-Peña, R. Advances in alkaline water electrolyzers: A review. *J. Energy Storage* **2019**, *23*, 392–403. [[CrossRef](#)]
8. Nikolaidis, P.; Poullikkas, A. A comparative overview of hydrogen production processes. *Renew. Sustain. Energy Rev.* **2017**, *67*, 597–611. [[CrossRef](#)]
9. Brauns, J.; Turek, T. Alkaline Water Electrolysis Powered by Renewable Energy: A Review. *Processes* **2020**, *8*, 248. [[CrossRef](#)]
10. Ulleberg, Ø. Modeling of advanced alkaline electrolyzers: A system simulation approach. *Int. J. Hydrog. Energy* **2003**, *28*, 21–33. [[CrossRef](#)]
11. Jupudi, R.S.; Zappi, G.; Bourgeois, R. Prediction of shunt currents in a bipolar electrolyzer stack by difference calculus. *J. Appl. Electrochem.* **2007**, *37*, 921–931. [[CrossRef](#)]
12. Colli, A.; Girault, H.H. Compact and General Strategy for Solving Current and Potential Distribution in Electrochemical Cells Composed of Massive Monopolar and Bipolar Electrodes. *J. Electrochem. Soc.* **2017**, *164*, E3465–E3472. [[CrossRef](#)]
13. Tang, A.; McCann, J.; Bao, J.; Skyllas-Kazacos, M. Investigation of the effect of shunt current on battery efficiency and stack temperature in vanadium redox flow battery. *J. Power Sources* **2013**, *242*, 349–356. [[CrossRef](#)]
14. Kim, S. Vanadium Redox Flow Batteries: Electrochemical Engineering. *Energy Storage Devices* **2019**. [[CrossRef](#)]
15. Hug, W.; Bussmann, H.; Brinner, A. Intermittent operation and operation modeling of an alkaline electrolyzer. *Int. J. Hydrog. Energy* **1993**, *18*, 973–977. [[CrossRef](#)]
16. Ulleberg, O. Stand-Alone Power Systems for the Future: Optimal Design, Operation and Control of Solar-Hydrogen Energy Systems. Ph.D. Thesis, Norwegian University of Science and Technology, Trondheim, Norway, 1998.
17. Tijani, A.S.; Rahim, A.A. Numerical Modeling the Effect of Operating Variables on Faraday Efficiency in PEM Electrolyzer. *Procedia Technol.* **2016**, *26*, 419–427. [[CrossRef](#)]
18. Ben Makhloufi, A.; Hatti, M.; Taleb, R. Comparative Study of Photovoltaic System for Hydrogen Electrolyzer System. In Proceedings of the 6th International Conference on Systems and Control (ICSC), Batna, Algeria, 7–9 May 2017.
19. Tlili, N.; Neily, B.; Ben Salem, F. Modeling and Simulation of Hybrid System Coupling a Photovoltaic Generator, A PEM Fuel Cell and An Electrolyzer (Part I). In Proceedings of the IEEE 11th International Multi-Conference on Systems, Signals & Devices (SSD14), Barcelona, Spain, 11–14 February 2014.
20. Ganguly, A.; Misra, D.; Ghosh, S. Modeling and analysis of solar photovoltaic-electrolyzer-fuel cell hybrid power system integrated with a floriculture greenhouse. *Energy Build.* **2010**, *42*, 2036–2043. [[CrossRef](#)]
21. Li, C.-H.; Zhu, X.-J.; Cao, G.-Y.; Sui, S.; Hu, M. Dynamic modeling and sizing optimization of stand-alone photovoltaic power systems using hybrid energy storage technology. *Renew. Energy* **2009**, *34*, 815–826. [[CrossRef](#)]
22. Sarrias-Mena, R.; Ramírez, L.M.F.; García-Vázquez, C.A.; Jurado, F.; Sarrias-Mena, R. Electrolyzer models for hydrogen production from wind energy systems. *Int. J. Hydrog. Energy* **2015**, *40*, 2927–2938. [[CrossRef](#)]
23. Ribeiro, E.; Cardoso, A.; Boccaletti, C. Power Converters Analysis in a Renewable Energy Based Hybrid System with Hydrogen Storage. In Proceedings of the IET Conference on Renewable Power Generation (RPG 2011), Edinburgh, UK, 6–8 September 2011.
24. Onar, O.C.; Uzunoglu, M.; Alam, M.S. Dynamic modeling, design and simulation of a wind/fuel cell/ultra-capacitor-based hybrid power generation system. *J. Power Sources* **2006**, *161*, 707–722. [[CrossRef](#)]
25. Tjarks, G.; Stolten, D.; Lanzerath, F.; Müller, M.; Bardow, A.; Stolten, D. Energetically-optimal PEM electrolyzer pressure in power-to-gas plants. *Appl. Energy* **2018**, *218*, 192–198. [[CrossRef](#)]
26. Khalilnejad, A.; Sundararajan, A.; Sarwat, A.I. Optimal design of hybrid wind/photovoltaic electrolyzer for maximum hydrogen production using imperialist competitive algorithm. *J. Mod. Power Syst. Clean Energy* **2018**, *6*, 40–49. [[CrossRef](#)]

27. Tijani, A.S.; Yusup, N.A.B.; Rahim, A.A. Mathematical Modelling and Simulation Analysis of Advanced Alkaline Electrolyzer System for Hydrogen Production. *Procedia Technol.* **2014**, *15*, 798–806. [[CrossRef](#)]
28. Zhou, T.; François, B. Modeling and control design of hydrogen production process for an active hydrogen/wind hybrid power system. *Int. J. Hydrog. Energy* **2009**, *34*, 21–30. [[CrossRef](#)]
29. Schalenbach, M.; Carmo, M.; Fritz, D.L.; Mergel, J.; Stolten, D. Pressurized PEM water electrolysis: Efficiency and gas crossover. *Int. J. Hydrog. Energy* **2013**, *38*, 14921–14933. [[CrossRef](#)]
30. Liso, V.; Savoia, G.; Araya, S.S.; Cinti, G.; Kær, S.K. Modelling and Experimental Analysis of a Polymer Electrolyte Membrane Water Electrolysis Cell at Different Operating Temperatures. *Energies* **2018**, *11*, 3273. [[CrossRef](#)]
31. Scheepers, F.; Stähler, M.; Stähler, A.; Rauls, E.; Müller, M.; Carmo, M.; Lehnert, W. Improving the Efficiency of PEM Electrolyzers through Membrane-Specific Pressure Optimization. *Energies* **2020**, *13*, 612. [[CrossRef](#)]
32. Yodwong, B.; Guilbert, D.; Kaewmanee, W.; Phattanasak, M. Energy Efficiency Based Control Strategy of a Three-Level Interleaved DC-DC Buck Converter Supplying a Proton Exchange Membrane Electrolyzer. *Electronics* **2019**, *8*, 933. [[CrossRef](#)]
33. Guilbert, D.; Vitale, G. Improved Hydrogen-Production-Based Power Management Control of a Wind Turbine Conversion System Coupled with Multistack Proton Exchange Membrane Electrolyzers. *Energies* **2020**, *13*, 1239. [[CrossRef](#)]
34. Colli, A.; Bisang, J.M. Combination of Cumulative and Convergent Flows as a Means to Improve the Uniformity of Tertiary Current Distribution in Parallel-Plate Electrochemical Reactors. *J. Electrochem. Soc.* **2017**, *164*, E42–E47. [[CrossRef](#)]
35. Colli, A.; Bisang, J. The effect of a perpendicular and cumulative inlet flow on the mass-transfer distribution in parallel-plate electrochemical reactors. *Electrochim. Acta* **2014**, *137*, 758–776. [[CrossRef](#)]
36. Colli, A.; Bisang, J.M. Validation of Theory with Experiments for Local Mass Transfer at Parallel Plate Electrodes under Laminar Flow Conditions. *J. Electrochem. Soc.* **2012**, *160*, E5–E11. [[CrossRef](#)]



© 2020 by the authors. Licensee MDPI, Basel, Switzerland. This article is an open access article distributed under the terms and conditions of the Creative Commons Attribution (CC BY) license (<http://creativecommons.org/licenses/by/4.0/>).